Synthesis and Atomic and Electronic Structure of New Si−Ge−C Alloys and Compounds

J. Kouvetakis* and D. Nesting

Department of Chemistry and Biochemistry, Arizona State University, Tempe, Arizona 85287-1604

David J. Smith

Center for Solid State Science and Department of Physics and Astronomy, Arizona State University, Tempe, Arizona 85287-1704

Received April 20, 1998. Revised Manuscript Received June 22, 1998

The synthesis and characterization of completely novel binary and ternary alloy semiconductors and ordered phases based on C, Si, and Ge are discussed in this review. Metastable compound semiconductors with ordered structures, which include stoichiometric SiGe, Si_4C, Si_3GeC_4 (sphalerite), Ge_4C, $(Si_2Ge)C_x$, and $(Ge_2Si)C_x$ ($x = 5\%$), are described. Materials systems include diamond-structured silicon−germanium solid solutions with dissolved carbon ($Si_{1-x-y}Ge_xC_y$), monocrystalline $Ge_{1-x}C_x$ hybrids of Ge, and C-diamond and related Si-containing random alloy systems. The Si_4C and Ge_4C materials incorporate the corresponding tetrahedra that are linked together to form a diamond-cubic structure related to Si. The Si_3GeC_4 phase is related to sphalerite and $(Si_2Ge)C_x$ has a new $P\bar{3}m1$ structure formed by Ge−Si−Si ordering along the diamond ⟨111⟩ direction. These compounds offer the prospect of band gaps wider than that of Si; in some cases, the band gaps are expected to become direct. This report emphasizes an approach that combines novel precursor chemistries and modern deposition techniques (ultrahigh-vacuum chemical-vapor deposition) to develop heteroepitaxial, device-quality inorganic materials. Important highlights of recent research based on conventional deposition methods are also summarized.

Contents

Introduction

The degree of maturity that has been achieved in the development of SiGe alloys and SiGe/Si heterostructures and nanostructures is best illustrated by the numerous device applications and the introduction of SiGe processes to very large scale integration (VLSI) technologies. The recent results obtained in heterostructure engineering with the introduction of substitutional carbon in SiGe have established Si−Ge−C alloys as important semiconductor materials as well as stimulated intense interest in the development of new inorganic alloys and compounds based on Group IV elements.

Silicon carbide (SiC) with its various polytypes and the diamond-structured $Si_{1-x}Ge_x$ random alloy are the only known, thermodynamically stable systems among the group IV elements. Other crystalline alloys and compounds that incorporate exclusively the diamond-lattice semiconductors C, Si, Ge, and α-Sn had until recently remained unexplored. A major limitation for their formation is the large difference in covalent radii among these elements ranging from 0.77 Å for C to 1.40 Å for Sn. The corresponding lattice constants vary from 3.5 to 6.5 Å. Another limitation is that the diamond structure is stable at room temperature and normal pressures for Si and Ge, metastable for C, and only stable up to near room temperature for α-Sn. For these reasons, most Si−Ge−C alloys and ordered phases are considered metastable at best.

Despite this inherent metastabilty, intense efforts are under way to produce materials that might combine the unique and exciting properties that the group IV elements are known to possess. These properties include a wealth of technological applications (Si), the highest thermal conductivity (diamond), high hole mobility (Ge), and band gap variation between 5.5 eV (diamond) and 0.1 eV (α-Sn). The materials from C to Ge, including SiC and $Si_{1-x}Ge_x$, all have an indirect band gap, most with the direct gap higher than the indirect gap by >1 eV (C, SiC, Si). However, the direct band gap of Ge lies slightly above the indirect band gap and a transition to a direct band gap is anticipated for new systems

10.1021/cm980294b CCC: $15.00
Published on Web 09/11/1998

containing Ge.[1] The development of a direct-gap group IV compound would have far-reaching implications in the integration of microelectronics and optoelectronics, which requires the combination of a direct-band-gap material with Si.

From a technological perspective, the major issues that drive research aimed at the synthesis of new group IV materials are band-gap engineering and lattice matching with Si. Band-gap engineering has been applied previously to realize practical goals, such as the creation of light-emitting and laser diodes, faster transistors, and a host of other novel devices using III−V compounds and alloys. However, because recent advances in integrated microelectronics continue to rely on the unique properties of Si, the synthesis of band-gap engineered, epitaxial, and preferably lattice-matched heterostructures on Si are considered essential for future generations of high-speed devices. Research and development in this area has primarily focused on the Si−Ge equilibrium system where the complete miscibility of the elements allows formation of alloys with variable composition, band structure, and lattice constant.[2,3] Recently, there has been much interest and activity in other group IV combinations.

From a synthesis viewpoint, the most important challenge for formation of group IV alloys and compounds is the development of novel methods and metastable conditions that yield device-quality material with the desired composition and structure. Very recently, conventional deposition techniques based on strain engineering have made strong progress toward the generation of monocrystalline but dilute (low C content) $Si_{1-x}C_x$ and $Si_{1-x-y}Ge_xC_y$ epitaxial layers on Si.[4−6] Electrical and structural properties for limited compositions of these material have also been investigated.[7] Ongoing research is based on development of novel chemical methods in combination with modern deposition techniques to synthesize highly saturated metastable alloys.[8,9] A wide variation in composition is necessary to systematically study the effect of composition on band structure and lattice constant. These methods should also provide the means for epitaxial formation of new ordered structures based on the C, Ge, and Si constituents.

From a fundamental viewpoint, new group IV compound materials offer a number of unique challenges. For example, although some theoretical predictions based on random alloy structures suggest that the band gap and lattice parameter vary smoothly with composition,[10] other studies indicate that they do not behave as random alloys.[11] In fact, recent calculations and experimental observations indicate that the electronic properties of certain alloyed materials are highly complex and depend strongly on the local atomic arrangements within the crystal.

The scope of this report is primarily to describe ongoing research dealing with synthesis and structural and bonding characteristics of this new class of electronic materials, as well as investigations of their electronic and optical properties,. The work to be described includes metastable ordered phases and solid solutions in the Si−Ge, Si−Ge−C, Si−C, and Ge−C systems. Because basic research issues dealing with stoichiometric SiC and $Si_{1-x}Ge_x$ have now shifted away from solid-state chemistry and materials science areas toward the device arena, discussions related to these materials is limited.

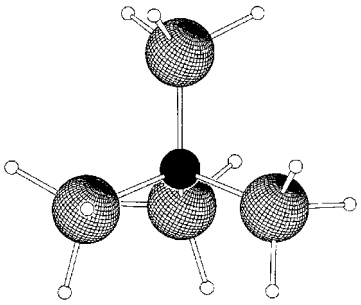

Figure 1. Molecular structure of $C(GeH_3)_4$ (*T* symmetry) as determined by gas-phase electron diffraction. The corresponding $C(SiH_3)_4$ molecule has essentially the same structure.

This review begins with a description of the preparation and structural analysis of simple inorganic cluster compounds, which are the crucial precursors that have led to the development of new group IV materials incorporating Ge_4C and Si_4C building units. The implications of the observed structural parameters for length and stability of Ge−C and Si−C bonds in crystalline semiconductor solids as well as the applicability of Vegard's Law to these systems are presented. Synthesis and properties of ordered phases (other than SiC) containing Si, Ge, and C and having diamond-like or sphalerite structures are described. Finally, recent studies oriented toward the growth and basic optical and electrical properties of technologically relevant, random alloy heterostructures are reviewed from a theoretical and experimental viewpoint.

Inorganic Compounds with Si_4C and Ge_4C Tetrahedral Cores

The diamond-like structure of solid solutions and compounds in the Ge−C, Si−Ge−C, and Si−C systems (C < 20 atom %) requires that the C atom is incorporated into the lattice as Si_4C or Ge_4C tetrahedra. Methods that utilize sources with multiple C−C and C−H bonds yield the thermodynamically stable SiC and graphite byproducts rather than the desired metastable products (see ref 5b). From a synthetic viewpoint, the most suitable building blocks should therefore consist of a central C atom surrounded by Si or Ge atoms, thus representing a fragment with diamond-like structure that is then terminated by H atoms. In addition, these compounds must be volatile to be employed in preparations involving chemical vapor deposition (CVD). The simplest of such compounds are $C(SiH_3)_4$ and $C(GeH_3)_4$ (see Figure 1).

A novel synthetic approach for development of new Si−Ge−C thin film materials on single-crystal Si by ultrahigh-vacuum (UHV) CVD has been developed and is based on reactions utilizing $C(SiH_3)_4$ and $C(GeH_3)_4$ as precursors.[8] In addition to their unique molecular structure, which incorporates the desired Ge_4C and Si_4C cores, there are several other important reasons for choosing these compounds as precursors: (a) the lack of strong C−H bonds allows low growth temperatures and thus promotes incorporation of high C concentration; (b) the encapsulation of C between four SiH_3 or GeH_3 ligands simplifies the formidable task of forming

Si−Ge−C materials by reaction of hydrocarbons with Si and Ge hydrides to a simple Si hydride−Ge hydride interaction; and (c) $C(SiH_3)_4$ and $C(GeH_3)_4$ are volatile solids (70 and 2 Torr, respectively, at 22 °C) and thus highly suitable for low-pressure CVD. Moreover, relative to other Si or Ge hydrides, they are nonpyrophoric and nonexplosive, and therefore easier to handle. These covalent cluster compounds have served as the first model for local carbon sites in Si−Ge−C crystals and related electronic materials based on the diamond structure. Most importantly, they provide a unique route to a new class of semiconductor materials as described in detail next.

Synthesis and Structures

$C(SiH_3)_4$ is a strain-free molecule with normal Si−C bond lengths. It is usually prepared via a rather complicated, multistep procedure described by Schmidbaur (see refs 12b−12e for related compounds).[12] On the other hand, $C(GeH_3)_4$ is readily prepared by $LiAlH_4$ reduction of the corresponding halides $C(GeBr_3)_4$ and $C(GeCl_2Br)_4$ which, in turn, are prepared by a single-step insertion of GeX_2 into the C−Br bonds of CBr_4 as illustrated in the following equations:[13]

$$4GeX_2\cdot\text{dioxane} + CBr_4 \rightarrow (X_2BrGe)_4C + 4\ \text{dioxane} \qquad (X = Cl, Br)$$

$$(BrX_2)_4Ge \xrightarrow[-LiX,\ -Al_3]{LiAlH_4} (GeH_3)_4C$$

The sterically crowded $C(GeBr_3)_4$ and $C(GeCl_2Br)_4$ clusters display physical and structural properties that are indicative of highly symmetric species with remarkably strained C centers. The structure of crystalline $C(GeBr_3)_4$ is distorted in the solid state with an average arrangement close to icosahedral symmetry. The derived Ge−C distance of 2.05 Å is substantially longer than the normal Ge−C bonds, which are close to 1.93−1.94 Å in carbogermanes. A precise molecular structure determination of $C(GeBr_3)_4$ (with *T* symmetry) by gas-phase electron diffraction, as shown in Figure 2, confirms that this elongation is symptomatic of a weakened bond presumably due to strain.[14] It should be apparent from Figure 2 that the positions of the outer 12 Br atoms are close to the vertexes of a regular icosahedron. The icosahedral arrangement seems to maximize the Br−Br distances and thus relieve repulsion and strain.

The unusual Ge−C bond length found in $C(GeBr_3)_4$ suggests that crystals with a C atom bonded to four Ge groups might be sterically very crowded. The idea of steric strain causing stretched bonds and reducing the stability of tetrahedral structures in the molecular and solid state is not new but nevertheless important with regard to structural characterization and theoretical modeling of Ge−C and Si−Ge−C semiconductors. Recent theoretical ab initio investigations[15] revealed that the Ge−C bonds at random substitutional sites of C in Ge must be stretched to accommodate strain. A typical bond length is reported to be 2.046 Å. This value is in remarkable agreement with the experimental value of 2.05 Å obtained for the strained $C(GeBr_3)_4$. Bond

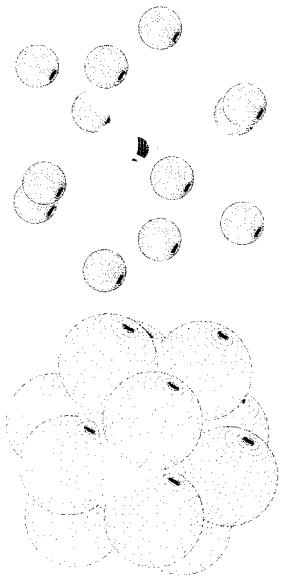

Figure 2. (Top) Molecular model of $C(GeBr_3)_4$ with *T* symmetry. (Bottom) Packing model of Br atoms in $C(GeBr_3)_4$. Each Br has five neighbors in an icosahedral arrangement.

lengths in the solid binary compounds consisting of C, Si, and Ge have been investigated using both the empirical Tersoff potential[16] and a self-consistent plane-wave technique.[17] Simulated concentrations AC, A_7C, AC_7, $A_{63}C$, and AC_{63} (where A = Si, Ge) with the diamond structure show that the Si−C and Ge−C bond lengths are highly dependent on the concentration of C in the compound. For the concentrations A_7C and $A_{63}C$, in particular, the calculated AC bonds are 4−8% longer than in the AC solid.

Interestingly, the structure of $C(GeH_3)_4$ demonstrates that there is very little strain associated with an isolated Ge_4C tetrahedral cluster terminated by H atoms. Based on a model of *T* symmetry, the structural determination gives a Ge−C bond length of 1.97 Å, which is slightly longer than normal but substantially shorter than that of $C(GeBr_3)_4$.[18] The rather short Ge−C bond length is surprising because $C(GeH_3)_4$ was predicted to be unstable, or at best a highly strained molecule because of steric Ge−Ge nonbonded interactions.[19] In fact, it is stable and its structure implies that a range of values are possible for Ge−C bond lengths. The experimental and theoretical evidence suggest that unusual Ge−C bond lengths should be possible in the tetrahedrally bonded materials described later.

To further demonstrate the implications of these results on bond length and stability in Ge−C crystals and related electronic materials, the structure of $C(GeBr_3)_4$ is compared with an element of a crystal structure derived by ordering of the diamond structure. The case considered is that of a simple ordered phase, AB_4D_3, which represents a possible structure for the composition Ge_7C [A = C (carbon), B = D = Ge]. Figure 3 shows a fragment AB_4D_{12} [= $A(BD_3)_4$] of this structure having a central atom A at the center of a cubic unit cell with symmetry $P43m$ (note that this is the same structure as the new spalerite-like $SiGe_3C_4$ described later). The next 12 D nearest neighbors of the central A atom are at the vertexes of a cuboctahedron. As shown in the figure, rotation of triangular C_3 groups about the B−D

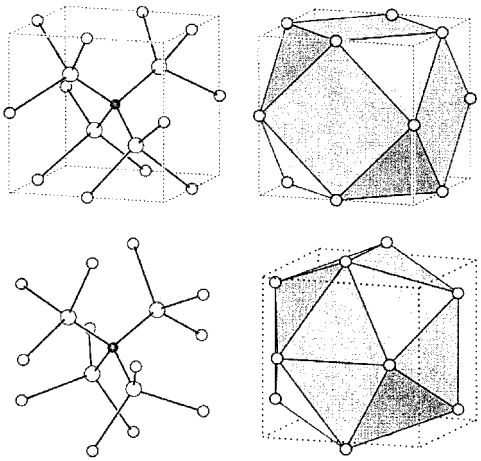

Figure 3. (Top) Left: a $P43m$ unit cell of an AB_4D ordered version of the diamond structure; right: the cuboctahedral arrangement of the D atoms shown at left. (Bottom) Left: $A(BD_3)_4$ molecule with the geometry of $C(GeBr_3)_4$; right: the icosahedral arrangement of the D atoms.

bond axis can convert the structure from a cuboctahedron to an icosahedron. This conversion illustrates that the crystal contains $A(BD_3)_4$ units but the constraints of symmetry require the more strained cuboctahedral geometry (with Td symmetry for the AB_4D_{12} fragment) in contrast to the molecule with icosahedral shape (T symmetry). Accordingly, Ge−C bonds even longer than 2.05 Å might be expected in diamond-related $Ge_{1-x}C_x$ crystals. Moreover, these observations cast serious doubts on the assumption that materials of Ge, or even Si, alloyed with C should obey Vegard's Law.

Finally, the validity of Vegard's Law in estimating the Ge−C composition that would allow Ge, SiGe, or Si doped with C to match exactly the lattice parameter of Si and thus allow strain-free heteroepitaxial growth is considered. According to Vegard's Law, the lattice parameter of an intermediate alloy phase may be obtained by linear interpolation between those of the two constituents. Assuming linear interpolation between the unit-cell parameter of C (diamond) and Ge, a ratio of Ge:C ratio of 8.5:1 would provide a match to the lattice parameter of Si. A normal Ge−C bond length of 1.93 Å would result in a unit cell constant $a = 4.492$ Å for the unknown GeC. Linear interpolation between GeC and Ge would give lattice matching with Si at Ge:C of 9.2:1. On the other hand, a Ge−C bond length of 2.05 Å gives $a = 4.734$ Å for GeC and the matching composition is then Ge:C of 7.1:1. Clearly, if linear interpolations remains valid, then the relationship between unit cell size and composition in Ge−C and Si−Ge−C alloys must be uncertain. It will become apparent from the specific material systems discussed later that the measured lattice parameters are larger than expected from Vegards' Law, a discrepancy that must be attributed to bond elongation.

Procedures for Growth and Characterization

The growth of most materials described here has been carried out in a simple custom-built UHV CVD system.[8] The single-crystal (100) Si substrates were first RCA-prepared in a clean room and then treated with 10% Hartree−Fock (HF) to passivate their surface. The

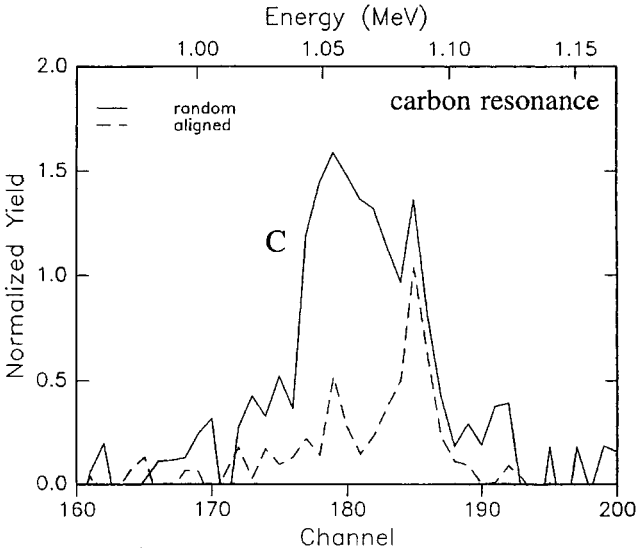

Figure 4. Carbon signals from the C-resonance RBS spectrum of $Si_{1-x-y}Ge_xC_y$ ($y = 0.02$; dotted line: aligned, solid line: random). The sharp surface peak does not show any ion channeling, whereas the bulk peak channels remarkably well, indicating that C primarily occupies lattice sites.[41]

passivating layer was removed at 450 °C in the reactor, and shortly thereafter the reactants were introduced into the reactor intermixed with large excesses of ultrahigh purity H_2. The interaction of SiH_4 and GeH_4 with $C(SiH_3)_4$ and $C(GeH_3)_4$ at 450−500 °C on the Si surface provides formation of films that are visually indistinguishable from the underlying substrate (experimental details for synthesis of each material system described in this report are referenced to published work in the following sections).

Several characterization techniques have been used to determine structural, compositional, and bonding properties of the thin film heterostructures, including the following: (a) High-resolution electron microscopy has been used for microstructural characterization, in particular to determine the quality of epitaxial growth. (b) Rutherford backscattering spectroscopy (RBS) has provided elemental composition, as well as estimates of film thickness and the quality of epitaxial growth using ion channeling. The Si−Ge elemental concentrations were obtained by utilizing 2 MeV He^{2+}, ions and the C content was measured with a C-resonance $^{12}C(\alpha,\alpha)^{12}C$ reaction at 4.265 MeV. To determine the location (substitutionality) of C in the diamond lattice, the C-resonance random and aligned spectra were compared, as shown for a representative sample in Figure 4. The C spectra clearly shows the presence of a nonsubstitutional surface C peak followed by a marked reduction of the signal inside the film, indicating that C is indeed part of the diamond lattice. (c) Secondary ion mass spectrometry (SIMS) has been used for qualitative and quantitative depth profiling as well as identification of the surface elements. (d) Fourier transform infrared spectroscopy (FTIR) and high-resolution Raman spectroscopy have been used to identify the local bonding environment of C atoms in the diamond-like lattice, the nature of possible precipitates, and to investigate strain. To determine whether C is entirely substitutional, FTIR and Raman spectra are routinely recorded, as shown by the example in Figure 5, which originates from the Si_2GeC_x ($x \sim 6\%$)

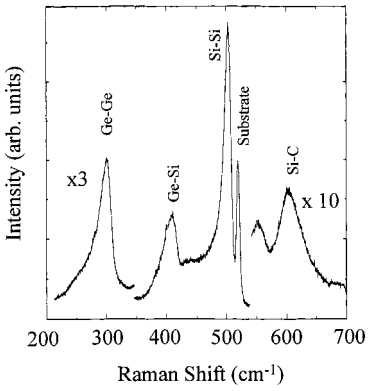

Figure 5. Raman spectrum of Si_2GeC_x (x = 6 atom %). In addition to Raman modes associated with the alloy, the Raman signal from the substrate is also visible at 520 cm^{-1}. Note the Si−C lattice mode at 607 cm^{-1} corresponding to substitutional C.

material described later. The spectra typically display a weak absorption at 607 cm^{-1}, corresponding to the localized mode of substitutional C in Si. Substitutional C in Ge is confirmed by a sharp absorption at 516 cm^{-1}. Strong absorption peaks at 800 cm^{-1} that would correspond to SiC are not usually observed. Nearly all of the materials described here have structures closely related to that of Si. They incorporate Si−C and Ge−C bonds substantially stretched relative to β-SiC, which are identified from a single three-dimensional local mode of *Td* symmetry at frequencies that are strikingly different from the vibrational frequency of the Si−C bond in β-SiC.

Group IV Semiconductor Compounds

Ordered structures composed of Si, Ge, and C offer the possibility of strain energy minimization by ordering the constituents in the same way that 50 atom % Si and 50 atom % C are ordered in the thermodynamically stable zinc blende SiC phase. In fact, in its various polytype forms, SiC is the only known stoichiometric phase among the elements C, Si, Ge, Sn, and Pb. In recent years, considerable effort has been devoted to preparation of an ordered stoichiometric SiGe phase because of its potential importance as a direct gap semiconductor. The first successful attempt to synthesize ordered SiGe was reported by Ourmazd and Bean in 1985,[20] and it has been since observed by many others in strained $Si_{1-x}Ge_x$/Si multilayers.[3,21]

Recent theoretical investigations have considered related hypothetical Si−Ge−C ordered structures with the diamond, zinc blende, Cu−Au, Cu−Pt, chalcopyrite, and luzonite [$Cu_3(As,Sb)S_4$] crystal structures.[22] With the exception of zinc blende SiC, all compounds considered were thermodynamically forbidden, although several showed promise for synthesis. It was reported that the most stable compounds were those that have C on a common sublattice and were nearly lattice-matched with β-SiC.

In this section we describe synthetic routes, structural characteristics, as well some other basic properties of selected strain-stabilized or unstrained (lattice-matched) diamond-cubic and zinc blende ordered phases from the Si/Ge, Si/C, Si/Ge/C, and Ge/C systems. The common feature of those that contain C is that C occupies one sublattice with Si and Ge on the other, so that only the closely matched Si−C and Ge−C bonds are present.

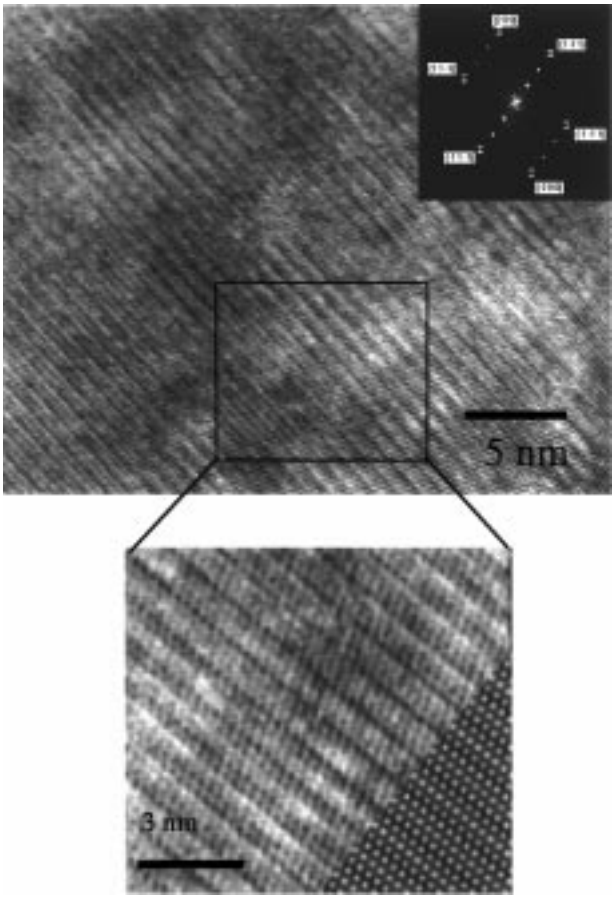

Figure 6. High-resolution electron micrograph of the (Si_2Ge)-C_x ordered structure deposited on (100) Si. Diffraction pattern (inset) corresponds to entire layer. Note diamond-cubic host reflections marked by frames and labeled with Miller indices. Superlattice spots indicating tripling along ⟨111⟩ directions are located between spots marked. A magnified section of the electron micrograph (below) is compared with image simulation of ordered structure (right corner).

Hexagonal Si_2Ge and Ge_2Si Structures

Si_2GeC_x. An unusual ordered Si_2Ge phase was observed recently in thin epitaxial layers of approximate composition Si_2GeC_x ($x \sim 6$ atom) grown on (100) Si. Except for regions near the interface, the ordered phase forms throughout the layer[23] by reactions of $C(SiH_3)_4$ with mixtures of SiH_4 and GeH_4. Electron microscope examination shows a periodic superstructure that has a periodicity along the ⟨111⟩ direction that is three times larger than that of the underlying Si lattice. Typical regions are shown in Figure 6. Selected-area electron diffraction patterns clearly show additional superlattice spots that correspond to the tripling of the {111} periodicity. Vibrational spectroscopic studies indicate that the C is completely substitutional with four Si atoms as nearest neighbors, consistent with the incorporation of the entire Si_4C tetrahedron into the Si−Ge−C lattice. The measured (111) lattice spacing of 3.15 Å is very close to the corresponding lattice spacing of Si (3.14 Å). The close matching is consistent with incorporation of substitutional carbon in the Si−Ge lattice.

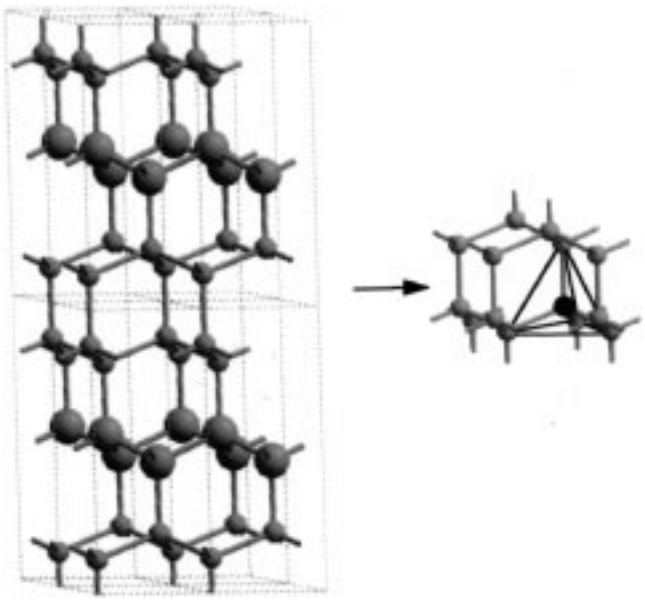

Figure 7. Illustration of ordered diamond structure of $(Si_2Ge)C_x$. Only Ge and Si atomic planes are shown. These are depicted by one layer of large blue spheres and two layers of small orange spheres respectively, stacked along the vertical direction. A possible C site (small dark sphere) and corresponding Si_4C tetrahedron (marked) are also shown inset in the Si bilayer.

Based on the observations of the superlattice structure, ab initio quantum mechanical modeling led to a proposed Si_2Ge structure with symmetry $P\bar{3}m1$, as shown in Figure 7. In this structure, a plane of atoms, presumably dominated by Ge is followed by two planes of Si atoms doped with C. Lattice coordinates determined with the empirical many-body potential of Tersoff[16] give a hexagonal unit cell with parameters a = 3.891 and c = 9.530 Å. There are two kinds of Si atoms: Si(1) atoms are located at ±(0, 0, 0.1237) and bonded to four Si atoms (some of these Si atoms are replaced by C to give the true $(Si_{2-x}Ge)C_x$ material); and Si(2) atoms at ±(1/3, 2/3, 0.7972) are bonded to three Si and one Ge. Finally, the Ge atoms at ±(1/3, 2/3, 0.5454) are bonded to one Si and three Ge. Of interest is the fact that the rhombohedral subcell of Si_2Ge, which would correspond to the cubic cell in the disordered phase, has a = 5.503 Å and α = 90.01°. The Si_2Ge structure was also confirmed by comparing computer-simulated images with experimental micrographs. Matching between calculated and experimental images is shown at the bottom of Figure 6. The calculated diffraction data for the Si_2Ge structure appear to be in excellent agreement with the experimental results and support the proposed ordered layering for this composition.

In contrast to this observation of extensive ordering in Si_2GeC_x, the absence of any ordering in samples of composition Si_2Ge implies that C must have played a role in this ordering. There is strong evidence that use of the $C(SiH_3)_4$ precursor results in C being incorporated into the structure as integral Si_4C units, immediately imposing substantial short-range order on the structure. Notice that in the proposed ordered structure, Si(1) atoms are surrounded by four Si atoms, so it is natural to assume that this is the preferred site for incorporation of C. Furthermore, incorporation of Si_4C tetrahedra clearly requires formation of at least two adjacent lattice planes that consist of Si atoms connecting the randomly distributed Si_4C units.

Ge_2SiC_x. The possibility of similar ordering in the corresponding $(Ge_2Si)C_x$ system was also investigated. Samples with approximate composition 7% C, 31% Si, and 62% Ge, corresponding to the desired $(Ge_2Si)C_x$, were readily obtained from the reaction of $C(SiH_3)_4$ with GeH_4 at 500 °C. This material was epitaxial and nearly monocrystalline, and the microstructure observed in cross section was dominated by {111} lattice fringes of the disordered phase. However, regions were observed that displayed a 3-fold periodicity along the ⟨111⟩ direction similar to that observed in $(Si_2Ge)C_x$. Because the compositional and vibrational data indicated that C is incorporated in the form of Si_4C units, it was inferred that the tripling of the lattice was again due to a Ge atomic layer followed by two layers consisting of Si_4C tetrahedra linked by Ge atoms rather than Si atoms as proposed for the $(Si_2Ge)C_x$ system. Computer-simulated images for a model based on a $Ge-(Si_{0.5}Ge_{0.5})-(Si_{0.5}Ge_{0.5})$ sequence appeared to be consistent with the experimental micrographs for $(Ge_2Si)C_x$. Furthermore, the lattice spacing of the "ordered" areas was slightly smaller than that of the disordered regions, implying that a larger concentration of Si_4C building blocks was incorporated into the ordered areas, thereby imposing short-range order.

$GeSi_3C_4$ with the Sphalerite Structure. In contrast to the compounds just described, the most promising structures in terms of lower energy do not match dimensionally with Si but match rather well with SiC. Although these structures are unstable with respect to decomposition into the constituent elements and SiC, metastable synthesis may again be possible using low-temperature growth techniques. For example, using nonequilibrium methods, the synthesis of a new Si−Ge−C compound with composition $GeSi_3C_4$ and a structure related to ZnS sphalerite was demonstrated.[24] This material was obtained by thermal decomposition (650−750 °C) of $(SiMe_3)_4Ge$, which is a remarkably volatile, air-stable compound, via elimination of benign byproducts such as CH_4, H_2, and $HSiMe_3$. Films ranging in thickness from 1000 to 5000 Å were deposited on single-crystal (100) Si and SiO_2 wafers. Extensive compositional and structural analysis revealed that this was a single-phase material containing Ge−C bonds, which are ordinarily disfavored in the crystalline solid state. Diffraction measurements gave a lattice constant slightly higher (by 1%) than that of cubic SiC, which is consistent with the larger Ge atoms substituting for Si atoms in the sphalerite structure. Vibrational studies (IR, Raman) revealed Si−C and Ge−C absorptions that were indicative of the zinc blende structure.

The diffraction data and phase composition suggested an ordered structure, as shown in Figure 8, where the Ge and Si atoms occupied the corner and face-centered positions, respectively, and C atoms occupied one-half of the tetrahedral sites of the face-centered-cubic unit cell. Independently, it has been predicted that $GeSi_3C_4$ is a low-energy structure nearly lattice-matched to SiC (mismatch of 1%), and it should also be a direct-band-gap semiconductor, although the optical transition strength may be small.[22] This cubic structure is de-

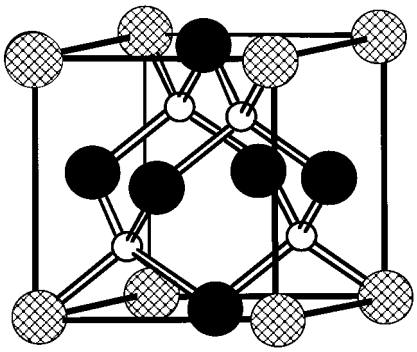

Figure 8. Zinc blende-based crystal structure of Si_3GeC_4. Shaded spheres at corners and dark spheres at faces represent Ge and Si atoms, respectively. Small spheres at T_d sites represent C atoms.

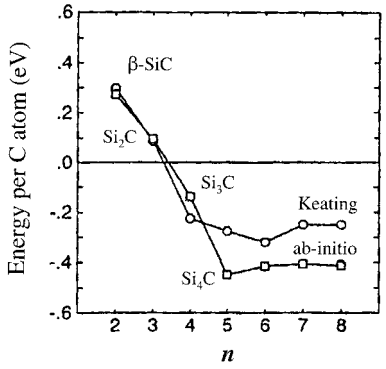

Figure 9. Energy per C atom relative to isolated substitutional C for range of $Si_{n-1}C$ structures that are strained to match the lattice of Si. The ab initio data are for the relaxed positions obtained from the Keating model.[25]

scribed as that of Luzonite, $Cu_3(As,Sb)S_4$, but in fact, this mineral has a different tetragonal structure.

Si_4C: A Binary Diamond-Like Phase. An ordered Si_4C structure that consists of Si_4C tetrahedra linked at the corners by Si−Si bonds has been predicted.[25] In theory, it is energetically preferred to a random alloy (0.4 eV per C atom) in comparison with isolated substitutional C atoms (see Figure 9). The C atoms in the lattice are arranged as third-nearest neighbors to allow the relatively short Si−C bond to exist with minimum strain. A model of the structure (not stabilized by strain) was obtained by the Tersoff method.[16] Refinement revealed a tetragonal unit cell ($I4_1/a$) with lattice constants $a = 7.793$ Å and $c = 5.029$ Å, as illustrated in Figure 10.[26] The lattice parameter of the pseudocubic cell is 5.029 Å. Osten and co-workers[25] have postulated that synthesis of such a highly concentrated Si−C diamond-cubic phase is only possible as a strained pseudomorphic layer embedded between pure crystalline Si layers. Related semiconductor structures that are not found in the bulk phase diagrams have been previously shown to be stabilized by substrate-induced strain.[27,28] A strain-stabilized Si_4C layer would, however, require stretching by at least 7−8% in the x,y plane of growth and should have very limited critical thickness. For thicker layers, strain relief by the formation of extensive defects and β-SiC should be expected.

Si/Si_4C/Si layered structures prepared via molecular beam epitaxy (MBE) were found to be epitaxial and crystalline.[25] The "Si_4C" layer was very thin (<10 Å)

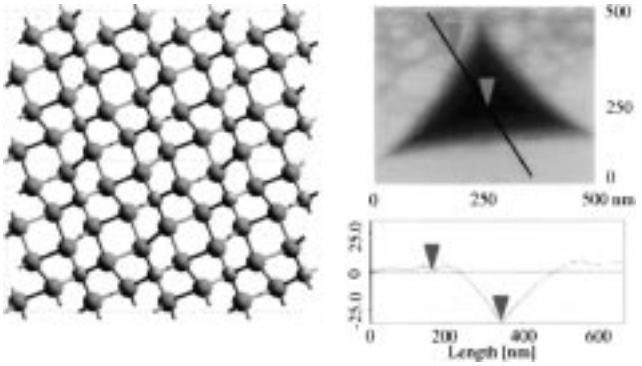

Figure 10. Left: The structure of Si_4C as projected on the $a-b$ plane for clarity. The Si_4C tetrahedra (Si atoms are orange spheres and C atoms are gray) are linked together so that C atoms are arranged as third nearest neighbors. Right: Typical microindentation atomic force microscopy (AFM) image and indentation depth profile that yields a hardness slightly higher than that of pure Si.

and thus difficult to analyze and characterize. Recently, a C-rich secondary phase was detected in an alloy material that had an overall composition of $Si_{89}Ge_{10}C_1$.[29] In regions where this phase was observed, a reduction in lattice spacing was measured along the vertical growth direction consistent with a cubic material stretched in the plane. The lattice parameter of this secondary phase was best explained by a model based on C atoms arranged as third-nearest neighbors (i.e Si_4C-related).[29]

A novel approach for synthesis of pure Si_4C layers that are sufficiently thick to allow complete characterization has focused on the thermal dehydrogenation of $C(SiH_3)_4$ on clean Si surfaces:

$$C(SiH_3)_4 \rightarrow Si_4C + 6\ H_2$$

This compound appears to be ideal for this purpose because it already incorporates the tetrahedral building block required to develop an extended Si_4C network.

A material having $Si_{80}C_{20}$ composition was deposited from $C(SiH_3)_4$ in the presence of H_2 at temperatures ranging from 550 to 700 °C.[30] The $Si_{80}C_{20}$ elemental content was the same as the Si:C ratio in the source precursor, implying that the composition and potentially the tetrahedral structure of the Si_4C core had been retained in the solid state. As-deposited material did not contain hydrogen and was completely amorphous, as shown in Figure 11. Annealing at temperatures <750 °C showed partial crystallization at the substrate alloy interface, whereas annealing at temperatures in the range 800−850 °C led to complete crystallization across the entire layer thickness via solid-phase epitaxy (see Figure 11b). The material was single-phase with the diamond-cubic structure (no evidence for SiC or C precipitation was found), although lattice defects were observed. Diffraction studies indicated a lattice constant ranging locally from ~0.5.35 to ~5.30 Å. This value is lower than that of Si (5.46 Å) but significantly higher than the value of 5.06 Å that would be calculated from Vegard's Law by assuming linear interpolation of the unit-cell parameters of diamond-C and Si. Analysis of the annealed samples confirmed that the composition had remained as Si_4C, and elemental depth profiles showed that the elements were still homogeneously

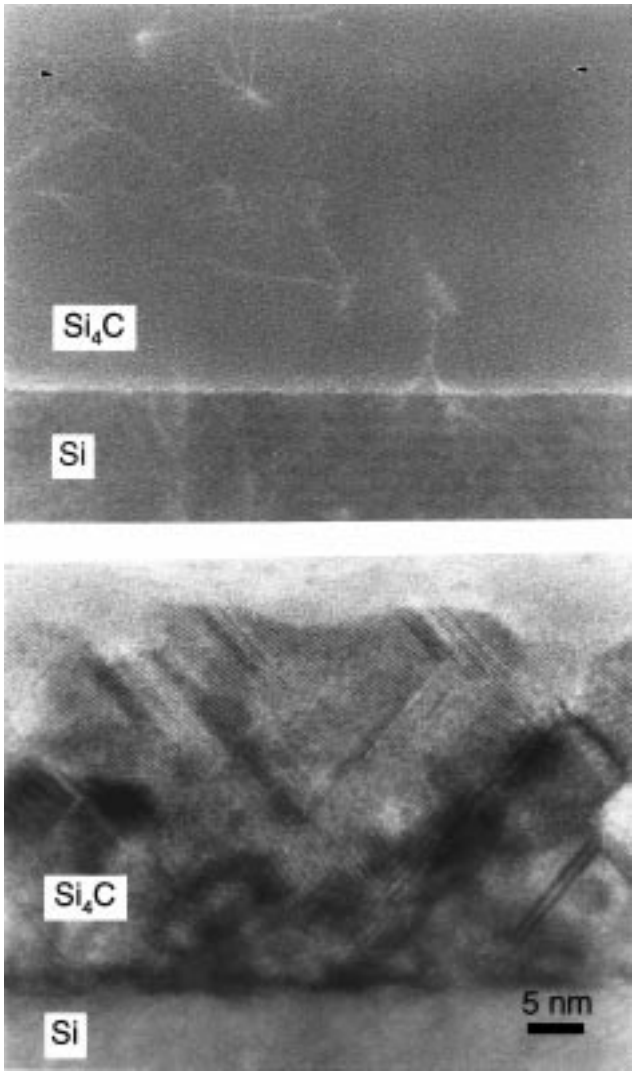

Figure 11. Cross-sectional electron micrographs of film with composition $Si_{0.80}C_{0.20}$: as deposited and completely amorphous (top); after annealing at 850 °C (bottom). Complete crystallization via solid-phase epitaxy has occurred across the entire layer thickness in the latter case.

distributed throughout the sample. At annealing temperatures >950 °C, nucleation of crystalline Si and β-SiC precipitates throughout the layer were observed, indicating the instability of the material at higher temperatures with respect to the thermodynamically stable products.

The $Si_{80}C_{20}$ material could only be grown as an epitaxial, crystalline layer to a maximum thickness of ~400 Å, above which the system became polycrystalline. Lattice parameters as low as 5.25 Å were measured in small grains, suggesting that the larger lattice parameter measured in the epitaxial layers may have been due to substrate-induced strain. Larger-than-normal Si−C bonds and possible strain stabilization of the crystalline $Si_{80}C_{20}$ are consistent with the proposed theoretical description of the structure. Vibrational characterization showed only the C−Si stretching mode at ~730 cm^{-1}. Comparison of this stretching frequency with that of cubic β-SiC at 800 cm^{-1} and the reported value[31] for the local vibrational mode in substitutional $Si_{1-x}C_x$ alloys at 610 cm^{-1} indicates that the Si−C bond is characteristic of a weakened bond, presumably due to strain arising from the sterically crowded Si environment. According to the proposed structure,[25] the stretched C−Si bond is 7% longer than the Si−C bond in β-SiC.

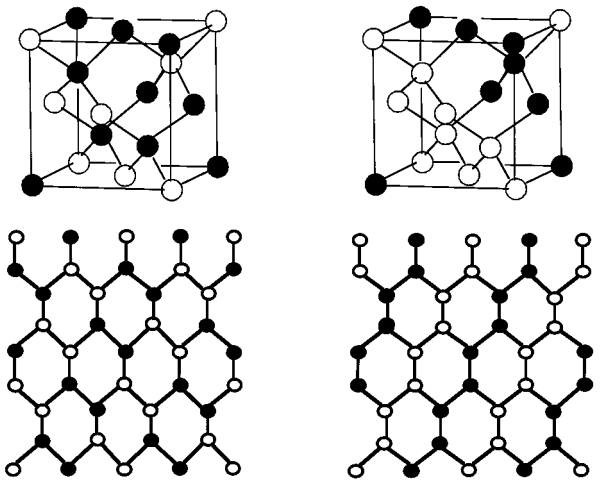

Figure 12. Models consistent with the proposed structure of SiGe. Top: one-eighth of the ordered unit cell (left: model proposed by Bean; right: model proposed by LeGoues).[33] Bottom: [101] projection through the unit cell.

Diamond-Cubic SiGe. Bulk Si and Ge form a continuous solid solution with diamond-cubic-type structure that has generally been accepted as an almost ideal solution. A recent extended X-ray absorption five structure (EXAFS) study of polycrystalline Si−Ge films annealed at 700 °C provided strong evidence for an essentially random alloy at all compositions.[32] Ordered phases in bulk Si−Ge have not yet been reported but short- and long-range order in stoichiometric SiGe grown under metastable conditions on Si substrates has been observed or suggested. Early reports indicate that annealing of strained layers formed on (100) Si by molecular beam epitaxy (MBE) yield an order−disorder transition in the SiGe sublayer.[20,21] The proposed structural model is based on a (SiGe)−(GeSi) sequence of atomic layers along the ⟨111⟩ direction, as shown in Figure 12**,** and corresponds to a fixed $Si_{0.5}Ge_{0.5}$ composition where three-fourths of the bonds are heteropolar (Si−Ge). It appears that this model is preferred over a zinc blende type in which all bonds (Si−Ge) are heteropolar.

Further investigations of the same $Si_{0.5}Ge_{0.5}$ composition by Le Goues and Iyer by Raman spectroscopy and electron diffraction confirmed the same ordering in unstrained layers, but an entirely different model was proposed.[33−35] In this case, the unit cell of the diamond-structured ordered phase is essentially doubled along the ⟨111⟩ direction (see Figure 12, top right). The ordering is described as alternating Ge and Si {111} lattice planes, where three-fourths of the bonds are homopolar (Si−Si, and Ge−Ge) and one-fourth are heteropolar (Si−Ge). This structure has been described as "microscopically strained" due to the difference in bond lengths, and its formation is justified in terms of its lower chemical energy. This energy was calculated by Martins and Zunger[27] and attributed to the higher number of homopolar Si−Si and Ge−Ge bonds that are considered stronger than the heteropolar Si−Ge bonds. Martins and Zunger[27] also determined that the lower chemical energy in this structure should compensate for

the higher mechanical energy that arises from strain, particularly because the latter was relatively small in Si−Ge alloys. The same argument was also used to explain why the model structure in Figure 12 (with 75% Si−Ge bonds) would be preferred over the zinc blende structure (with 100% Si−Ge bonds).

The strongest evidence for the structure proposed by Le Goues is obtained by high-resolution electron diffraction and resonant Raman studies. Determination of the exact structure was based on strong superlattice reflections observed in diffraction patterns collected along several zone axes. All superlattice reflections, including intensities, were compared with simulated diffraction patterns and found to be in exact agreement with the structure in Figure 12. The Raman spectra of the ordered phase were also recorded and compared with the spectrum of the corresponding random alloy. The changes in the relative intensities of the different optical phonon modes (Si−Si, Si−Ge, and Ge−Ge) were consistent with an ordered structure in which the majority of the bonds were homopolar and the minority were heteropolar. The Raman intensity changes support the proposed structure although the spectra also showed that ordering was always incomplete at ~60−65%.

Other phases in the $Si_{1-x}Ge_x$ system have been reported, although they appear to be less certain and not as thoroughly studied as the cubic SiGe. More recently, two coexisting ordered models have been proposed in a strained $Si_{0.6}Ge_{0.4}$ layer.[36] Based on extremely weak superlattice reflections in X-ray diffraction pattern, the atoms in the structure are purported to align in the sequences Ge−Si−Ge−Si and Ge−Si−Si−Si along the (111) axis. However, no microstructural data was provided to support the claim. A similar Ge−Si−Si−Si ordering has been proposed for isolated grains in a material with bulk composition $Si_{0.70}Ge_{0.30}$.[37] In all of these cases, the ordered phase is a minority component of the bulk material.

Group IV Semiconductor Alloys

The Si−Ge−C System. Alloys of $Si_{1-x}Ge_x$ have continuously variable lattice parameters and band gap, and they have attracted much attention because of their potential for numerous practical applications.[38] For example, they have been successfully used to create heterojunction bipolar transistors (HBTs) with cutoff frequencies in excess of 100 GHz, which is substantially higher than for the traditional Si counterparts.[39] For this reason, the Si−Ge system has been considered as the natural complement to silicon in high-frequency applications.[40]

A problem facing Si−Ge technology is the inherent 4% lattice mismatch between Si and Ge that causes compressive strain in $Si_{1-x}Ge_x$ layers grown heteroepitaxially on Si. The strain increases both with increasing Ge concentration as well as increasing Si−Ge film thickness. A possible solution to the mismatch problem is the incorporation of C which, in the diamond form, has a lattice constant of 3.57 Å, which is significantly smaller than those of Si (5.43 Å) and Ge (5.65 Å). Incorporation of C into SiGe material should reduce the lattice mismatch with the smaller size of C, compensating for the larger size of Ge. Using Vegard's Law, a Ge:C ratio of ~9:1 would in principle at least provide an alloy that is lattice-matched with Si. The incorporation of a third component also adds additional flexibility in band-gap engineering. Indeed, it has been suggested that the advent of high quality $Si_{1-x-y}Ge_xC_y$ material could push device performance into even higher frequency ranges, posing a challenge to GaAs technologies that have dominated the high-frequency market.[40]

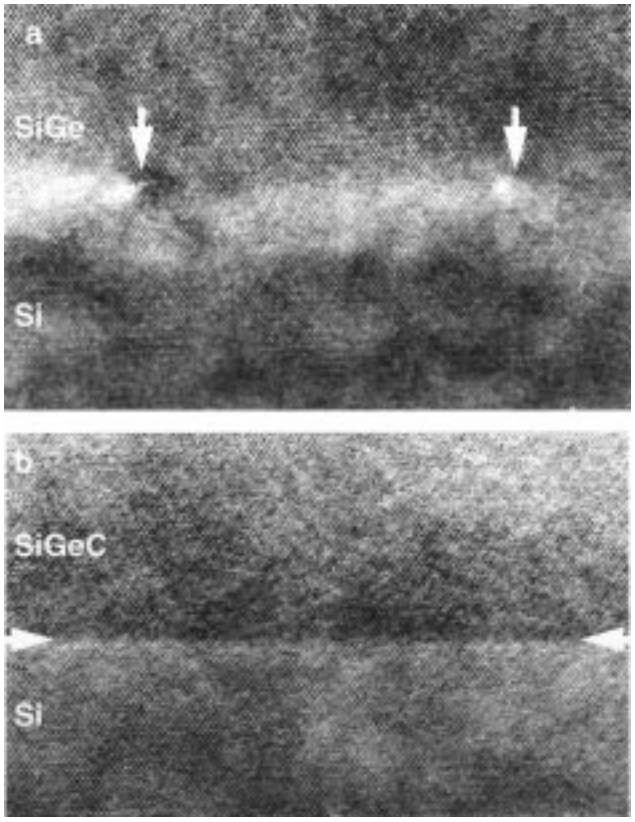

Figure 13. Cross-sectional electron micrographs: (a) Si/SiGe interface with misfit dislocations (arrowed); (b) Si/Si−Ge−C interface (arrowed) showing defect-free coherent growth.

The incorporation of C into SiGe has been the objective of much ongoing effort since the early 1990s using techniques such as MBE and solid-phase epitaxy, as well as conventional CVD. These attempts have typically resulted in maximum C incorporation levels of ~1−2 atom %, which allow a limited range of Si−Ge compositions under lattice-matched conditions. Recently, CVD processes using hydrocarbons with multiple C−H bonds, such as C_2H_2 and C_2H_6, as the source of C led to the development of device-quality material with 2 atom % C incorporation.[41] The addition of C was shown to have a marked effect on the structural quality of the material. Whereas defects such as misfit dislocations were usually observed at the SiGe/Si interface due to lattice mismatch, the new SiGeC films grown at 700 °C had very few interfacial defects, as shown in Figure 13.[42] Furthermore, the addition of C into the SiGeC lattice led to substantial increases in the critical thickness for defect-free epitaxial growth. Substitution of C into SiGe lattice has thus achieved reduction of the lattice mismatch between the SiGe layer and the Si substrate.

Despite the successful synthesis of device-quality, low-carbon-content Si−Ge−C films, it has been proven difficult to incorporate C in sufficient quantities to

achieve lattice matching, especially for large Ge concentrations. Continuing efforts to introduce >2 atom % C by conventional CVD require high deposition temperatures and have usually resulted in amorphous or at best polycrystalline materials. The low C incorporation is attributed to the high stability of the C−H and C−C bonds of the precursors. High reaction temperatures are required, which seem to favor SiC precipitation, phase separation, and inhomogeneous material. MBE studies confirm that the incorporation of substantial C into substitutional sites of the SiGe crystal lattice can only be accomplished by kinetically favored, low-temperature growth conditions (450−500 °C) in contrast to thermodynamically stable SiC, which is likely to form at high temperatures.[6]

Novel deposition methods are required that provide a higher degree of compositional control as well as favoring lower temperature reaction routes that could lead to novel metastable structures with the desired compositions. The primary objective is to develop alternative methods of creating highly concentrated layers (C > 4 atom %) that are inaccessible by conventional routes. Methods based on reactions of $C(SiH_3)_4$ and $C(GeH_3)_4$ with SiH_4 and GeH_4 have been successfully utilized to prepare Si−Ge−C materials with C contents substantially higher than obtained previously.

(i) $(Si_4C)_xGe_y$ and $(Ge_4C)_xSi_y$. Reactions of $C(SiH_3)_4$ with GeH_4 at 450 °C, and $C(GeH_3)_4$ with SiH_4 at 500 °C, yield materials with the general formulas $(Si_4C)_x$-Ge_y and $(Ge_4C)_xSi_y$, respectively.

$$C(SiH_3)_4 \xrightarrow[-H_2]{GeH_4} (Si_4C)_xGe_y$$

$$C(GeH_3)_4 \xrightarrow[-H_2]{SiH_4} (Ge_4C)_xSi_y$$

A range of $(Si_4C)_xGe_y$ compositions containing 3−10 atom % C was prepared. A typical sample having C = 5 atom %, (Si = 20 atom %, Ge = 75 atom %) was monocrystalline and epitaxial.[9] However, severe degradation of crystallinity and epitaxial quality occurred when the C content was increased to levels >7 atom % and samples with 10 atom % C were entirely polycrystalline. As shown in Figure 14, a typical sample of the $(Ge_4C)_xSi_y$ material with C = 5 atom %, (Ge = 20 atom % and Si = 75 atom %) was completely epitaxial and displayed better crystallinity and fewer defects than the corresponding $(Si_4C)_xGe_y$ sample with the same C concentration. The reactions of $C(SiH_3)_4$ and $C(GeH_3)_4$ with GeH_4, and SiH_4, respectively, demonstrate the successful preparation of single-phase material incorporating significant carbon (5−6%) content. They also indicate the remarkable degree of compositional control that these two compounds can provide by incorporating the composition of the Ge_4C and Si_4C molecular framework into the solid state.

(ii) $Si_{1-x-y}Ge_xC_y$. The reactions of $C(SiH_3)_4$ with various combinations of SiH_4 and GeH_4 was further explored to determine the optimum conditions for possible lattice matching. The objective was again to prepare $Si_{1-x-y}Ge_xC_y$ materials that incorporated wide variations in Si and Ge concentrations while maintaining the C content at a significant level in the 5% range. One aim of these experiments was to establish whether

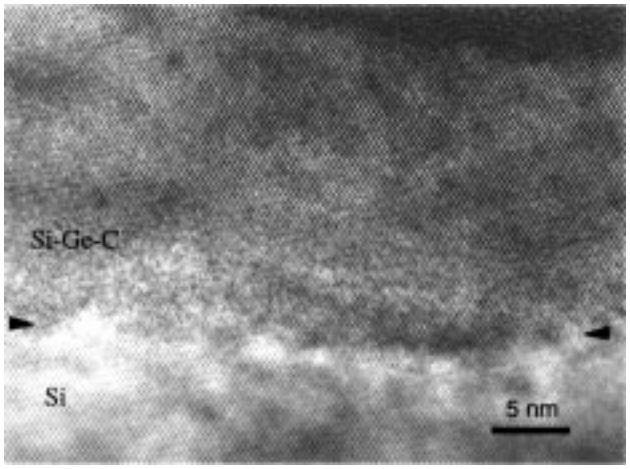

Figure 14. Cross-sectional electron micrograph showing heteroepitaxial growth of $(Ge_4C)_xSi_y$ ($y = 0.05$) obtained using $C(GeH_3)_4$ as the C source. Note relatively defect-free Si/Si−Ge−C interface. The crystal quality of materials obtained using $C(GeH_3)_4$ was better than those obtained from $C(SiH_3)_4$.

a Ge:C ratio of ∼9:1 would indeed afford lattice-matched material as predicted by Vegard's Law. By growing at 470 °C with a rate of 6 Å/min, $Si_{1-x-y}Ge_xC_y$ materials ($x = 0.31-0.34$ and $y = 0.03-0.07$) were produced that were nominally lattice-matched to Si. An SiGeC layer, with a nominal C content of 4−5 atom %, displayed a high degree of crystalline perfection, and the lattice constant (5.46 Å) matched closely with that of Si (5.43 Å). No evidence of SiC precipitation was observed, and the subtle decrease in the lattice constant of the diamond-cubic unit cell with increasing C content from 3 to 6 atom % was consistent with the smaller size of C substituting for the larger size of Ge in the lattice. The remarkably low deposition temperature undoubtedly favors incorporation of the C in the diamond lattice as indicated by a variety of analytical methods.

The GeC System. A major reason for continued interest in Ge−C alloys is the observation that the lattice parameter of Si (a = 5.43 Å) is intermediate between that of Ge (a = 5.657 Å) and diamond (a = 3.567 Å). A Ge film doped with a suitable level of C should exactly match the lattice parameter of Si, which would then allow growth of strain-free heteroepitaxial layers. This simple binary system offers the potential for band-gap engineering and, in theory, band gaps greater than those of Ge, Si−Ge, or even Si are expected with increasing C concentration. Wide band gap $Ge_{1-x}C_x$ superlattices would likely have important technological applications in high-speed heterojunction bipolar transistors and optoelectronics.[43] Surprisingly, although SiC is a well-known stable phase and Si and Ge form continuous solid solutions, the mutual solubility of C in Ge is very small and the compound GeC is predicted to be metastable with respect to disproportionation into the elements.[44] In fact, no inorganic crystal structure with the Ge−C bond appears to have been reported,[45] although metastable dilute solutions of C in Ge have been prepared recently by a variety of deposition and implantation methods. Antimony-mediated growth of epitaxial $Ge_{1-x}C_x$ hybrids of diamond and germanium (x = 1 atom %) have been prepared by MBE.[46] This method of surfactant (As,Sb)-mediated growth has been successfully applied to suppress island formation (Stran-

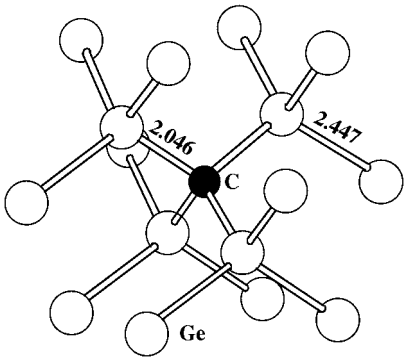

Figure 15. Structure of substitutional C in Ge calculated from ab initio theory.[15] The bond lengths are expressed in Angstroms.

ski-Krastanov mode) during growth of pure Ge layers on Si by artificially reducing the strain that exists between the lattice-mismatched Si and Ge. It was determined, however, that the $Ge_{1-x}C_x$ layer did not behave identically to pseudomorphic Ge and it should instead be considered as a new material with its own intrinsic strain properties. Several other synthetic studies by solid-source MBE have yielded strain-stabilized materials with reduced lattice constants and increased band gap relative to bulk Ge that are consistent with formation of a solid solution between diamond and germanium.[47]

A more recent investigation utilized implantation of C into single-crystal Ge followed by annealing at 350 °C to introduce a very minor concentration of substitutional carbon.[15] The substitutionality of C was confirmed by a sharp absorption in the IR spectrum at 516 cm^{-1}. This value is characteristic of a weak and rather elongated Ge−C bond and it is in good agreement with the calculated frequency of C impurities in Ge. The elongation was attributed to steric strain around the C lattice site. Complementary ab initio calculations were also performed to investigate the length and stability of the Ge−C bond. In these calculations, clusters of a central C atom are surrounded by either 34 or 70 Ge atoms forming a fragment of the diamond structure (*Td* symmetry). The Ge−C bond lengths were longer than normal, being 2.081 and 2.045 Å in the smaller and larger clusters respectively, as shown in Figure 15.

Highly Saturated $Ge_{1-x}C_x$ Incorporating Ge_4C Building Blocks. $C(SiH_3)_4$ and (to a lesser extent) $C(GeH_3)_4$ were successfully utilized to synthesize high carbon content, heteroepitaxial $Si_{1-x-y}Ge_xC_y$ alloys. The corresponding $Ge_{1-x}C_x$ materials are, however, much more difficult to prepare. The instability of the Ge−C bond (due to strain) is considered to be a dominating factor. Nevertheless, we have demonstrated that $C(GeH_3)_4$ is a highly effective precursor for low-temperature Ge−C growth.[48] The lack of strong C−H bonds favors lower deposition temperatures thus leading to novel metastable compositions. For example, the thermal dehydrogenation of the molecule at 500 °C on chemically clean (100) Si yields a new crystalline semiconductor that has Ge and C in the ratio of ∼4:1, according to the following equation. This ratio corresponds to the same atomic ratio as the precursor suggesting that the Ge_4C composition, and possibly the tetrahedral structure of the gaseous molecule, is retained in the solid state.

$$C(GeH_3)_4 \rightarrow 6H_2 + Ge_4C$$

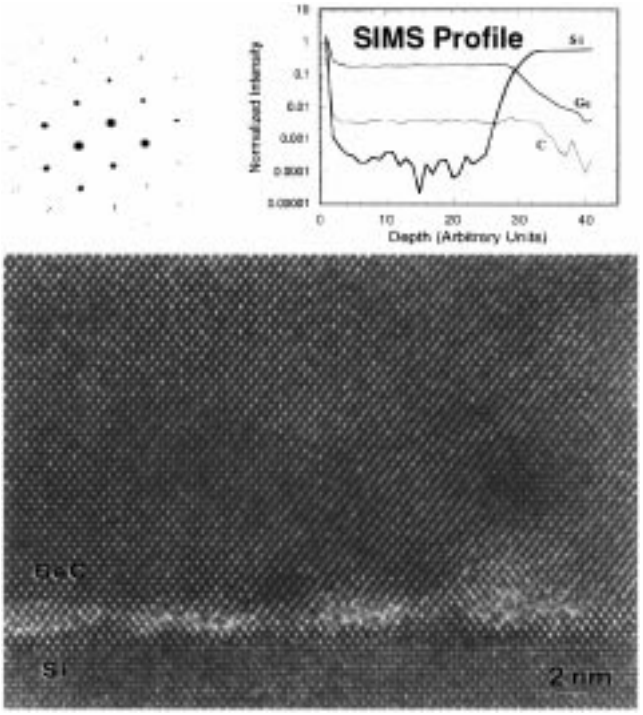

Figure 16. High-resolution electron micrograph showing cross-sectional view of heteroepitaxial $Ge_{0.98}C_{0.02}$. The electron diffraction pattern and the SIMS depth profile are also shown.

Structural analysis indicates that the deposited material has the diamond cubic structure and a lattice constant lower than that of Ge but substantially higher than the value calculated by Vegard's Law. Interactions of $C(GeH_3)_4$ (and analogous germylmethanes)[49] with GeH_4 or $(GeH_3)_2$ at 500 °C produced Ge−C materials with C compositions ranging up to 20 atom %. The $Ge_{1-x}C_x$ materials having C concentrations up to ∼3% were virtually monocrystalline and completely epitaxial. As shown in the high-resolution electron micrograph in Figure 16, the low deposition temperature and the relative low growth rate of 5−6 Å/min have yielded nearly perfect epitaxy, and allowed the formation of a remarkable layer of l000 Å thickness for a material that should be dominated by strain. The Ge−C samples with C content ranging from 2.5 to 6 atom % were crystalline and heteroepitaxial but, as shown in Figure 17, they showed a substantial concentration of {111} stacking faults and microtwins that originated from the Ge−C/Si interface and extended through the layer. The lattice constant of samples with composition $Ge_{94}C_6$ was 5.50 Å, about midway between those of Si and Ge. This value is again higher than the value calculated by Vegard's Law.

A noteworthy highlight of the Ge−C synthesis was the dramatic change in morphology and structure of the material with increasing C content. A decrease in growth rate with increasing C content from 3 to 5 atom % provided layer-by-layer growth that resulted in high-quality epitaxy and virtually atomically flat surfaces. This type of growth behavior is not observed for pure Ge deposition on Si. Novel defect-induced crystal growth of carbide nanorods occurred in samples with

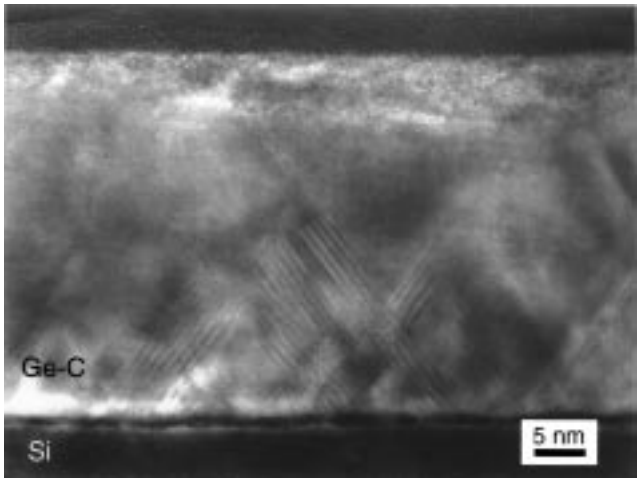

Figure 17. High-resolution electron micrograph showing smooth surface of heteroepitaxial $Ge_{0.95}C_{0.05}$.

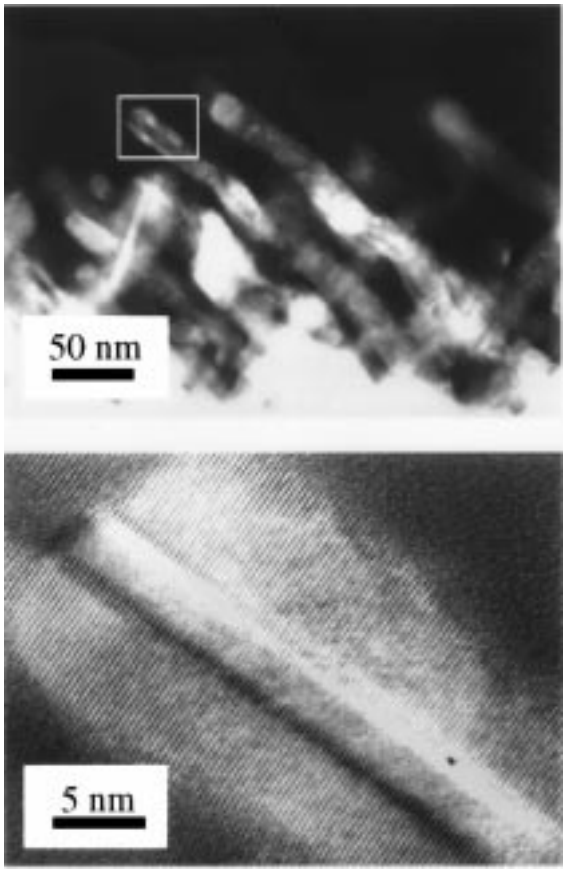

Figure 18. Cross-sectional view of monocrystalline C nanorods growing out from 400 Å $Ge_{1-x}C_x$ epitaxial layer. The C contents of the rods are higher that of the layer, and the lattice constant is considerably lower.

overall C content of ~13−15 atom % (see Figure 18). The lattice constant of these monocrystalline rods, which grew very rapidly from the surface of a 400 Å Ge−C layer, is ~5.46 Å, which is remarkably close to that of pure Si. These unstrained nanostructures offer the promise that a diamond-structured Ge−C material that matches dimensionally with Si may be possible.

The Si−C System. Carbon incorporation onto the substitutional sites in Si to create hybrids of C (diamond) and Si has attracted the most attention among the various group IV combinations described in this report. The $Si_{1-x}C_x$ alloys and strained superlattices are the focus of substantial ongoing academic and industrial research, particularly in the field of band-gap engineering. The principle again is that the lattice mismatch between the substrate and the deposited material can be accommodated by elastic strain, which directly influences the band structure. Furthermore, the formation of solid solutions between diamond and Si should also influence the band structure, and band gaps intermediate to those of Si and SiC are expected. From a synthesis viewpoint, the most difficult problems associated with the realization of device quality epitaxial superlattices of $Si_{1-x}C_x$ on Si are: the low solubility of C in Si; the enormous (52%) lattice mismatch between Si and C (diamond); and the high stability of stoichiometric SiC in its various polytype forms.

It has been known for decades that C impurities prefer substitutional sites in the Si lattice with a thermodynamic solubility limit of only 1×10^{-6} atom % C at the Si melting point.[50] This extremely low solubility is attributed to the large mismatch between the bond lengths of Si−Si (2.35 Å) and C−C (1.55 Å), which causes considerable strain around the C site and presumably results in elongation of the Si−C bond relative to the Si−C bond (1.89 Å) in zinc blende β-SiC. Substitutional carbon in Si is readily identified by IR or Raman spectroscopies from a single three-dimensional local mode at a frequency of 607 cm^{-1}.

Alloys of C with Si are unstable with respect to SiC. To avoid SiC precipitation, the synthesis of $Si_{1-x}C_x$ is possible under metastable conditions that can only be achieved by chemical and physical deposition methods and low temperatures. Once deposited as random alloy at ~450−550 °C, the material can then withstand higher annealing temperatures, such as 800 to 900 °C, a range that is compatible with Si processing technologies. Early attempts to prepare $Si_{1-x}C_x$ were reported[51] using remote plasma-enhanced CVD to fabricate 7-mm thick layers with C concentration of ~3.0 atom %. A noteworthy result of this study was that the lattice constant was higher than expected, which indicated that, unless there was some precipitation of SiC during growth, the material did not obey Vegard's Law. This work was followed by the development of a low temperature (500 °C) process that allowed synthesis of high quality epitaxial material and strained-layer superlattices stable up to 850 °C.[52] Comparable C concentrations were obtained by solid-source MBE.[53]

Substantial research is currently ongoing, and impressive results have been achieved in growing device-quality, thin superlattices and quantum wells using a variety of nonequilibrium growth processes such as CVD, MBE, and ion implantation followed by regrowth methods.[54] The effect of C concentration on the structure, strain, and band gap has been considered as well as stability versus temperature issues. Materials with C concentration ranging from 0.2 to 3.0 atom % typically consist of a single diamond-cubic phase and they have lattice constants significantly higher than predicted by Vegard's Law because of elongation of the Si−C bond. Furthermore, the materials were highly strained but always withstood annealing at higher temperatures. Between 800 and 900 °C, release of strain by interdiffusion was observed, whereas >900 °C, the layers

relaxed predominantly by β-SiC precipitation rather than formation of extended defect structures.

Highly Concentrated $Si_{1-x}C_x$ Based On Si_4C Building Blocks. The incorporation of high C concentrations (C > 3.0 atom %) are thus far inaccessible. An alternative synthetic approach of creating highly concentrated layers has utilized reactions of the Si−C sources, $C(SiH_2Cl)_4$ and $C(SiH_3)_4$ with either SiH_4 or $(SiH_3)_2$.[55] The major advantage of this configuration is that it provides Si_4C tetrahedral units that are structurally compliant with the desired $Si_{1-x}C_x$ diamond-like materials. Furthermore, the absence of strong C−H bonds permits substantially lower reaction temperatures, which are essential for growing metastable material and suppressing formation of the thermodynamically favored SiC in these highly saturated systems. A very recent study of $Si_{1-x}C_x$ deposition very clearly demonstrated that lower growth temperatures reduce the mobility of carbon on the surface during growth and considerably improve the substitutional carbon incorporation.[56]

Synthesis of Si−C random alloys with carbon compositions ranging up to 20 atom % was achieved at 600 °C using gas mixtures of SiH_4 with $C(SiH_3)_4$ or $C(SiH_2Cl)_4$. The final $Si_{0.80}C_{0.20}$ composition, described earlier, consists of interconnected Si_4C tetrahedra that form a diamond-like network in which the C atoms occupy a common sublattice. A very important result obtained by quantitative Raman measurements suggested that the substitutional C concentration obtained using this protocol is higher than concentrations obtained by other methods. Raman spectroscopy can be used to estimate substitutional C concentration using the shift of the Si−Si mode and the relative intensity of the C mode.[57] The Raman and IR spectra also show that the C local mode vibrational frequency increases with increasing C concentration, which is consistent with a decrease in bond length.[55] Materials that have relatively higher C, content such as Si_4C and SiC display higher vibrational frequencies at 730 and 800 cm^{-1}, respectively, and have relatively shorter Si−C length. This compositional dependence of the C mode can also be used to estimate C concentration if it is assumed that this mode would extrapolate for C = 50 atom % to the weighted average of the frequencies of β-SiC.

The effect of catalytic quantities of Ge on the growth characteristics and microstructure of the Si−C materials was also investigated in this study.[55] The objective was to exploit Ge-assisted growth to achieve lower deposition temperatures, increased growth rates, and the highest possible amount of substitutional C in the material. Moreover, it was anticipated that small Ge concentrations (<1 atom %) should serve to minimize strain in the system by reducing the lattice mismatch between $Si_{1-x}C_x$ and the Si substrate. The results confirmed that Ge incorporation indeed had a profound effect on the crystallinity and growth characteristics. In general, the Ge-doped samples were highly monocrystalline with some minor growth defects such as stacking faults, whereas the pure samples without Ge were highly defective. In addition, much more uniform growth and substantially higher growth rates were obtained in those depositions where Ge was used as the reactant.

Influence of Carbon on Band Structure

From an experimental and theoretical viewpoint, the current knowledge of optical and electrical properties of strained $Si_{1-x}C_x$ or lattice matched $Si_{1-x-y}Ge_xC_y$ alloys is still limited but a reasonable understanding of the effect of substitutional C on the band structure is evolving. Early theoretical investigation of $Si_{1-x}C_x$ and $Si_{1-x-y}Ge_xC_y$ band gaps by Soref,[10] using an empirical interpolation technique, predicted that the band gap of Si (1.1 eV) would increase dramatically with increasing C concentration. Alternatively, Sankey et al.[11] modeled $Si_{1-x}C_x$ alloys with supercells having random occupation of the lattice sites, and found that the fundamental band gap should be reduced by a small concentration of C in the Si lattice. In fact, the band gap is smaller than that of pure Si at ~10% C and such compositions were predicted to become metallic. This is a very unexpected result because both SiC and diamond have band gaps that are much wider than that of Si. It was eventually determined that the band structure of Si−C must be a complex function of alloy composition and strain effects. A similar conclusion was reached by Osten and coworkers[58] for both Si−Ge−C and Si−C random alloys containing only modest C concentrations. They find that current theoretical models cannot describe the behavior of optical transitions obtained experimentally in these systems.[58]

To adequately account for the observed energy shifts for pseudomorphic C-containing layers, both strain-induced effects and effects due to alloying have to be considered (the initial incorporation of substitutional into pseudomorphic $Si_{1-x}Ge_x$ has two separate effects on the band gap). Recent investigations of direct transitions and electrical properties suggest that the influence of C on band structure is not as significant as its effect on crystallographic structure.[59] Indeed, strain compensation and reduction of the lattice constant is now readily obtained as a function of increasing C content in the $Si_{1-x-y}Ge_xC_y$ system. A given $Si_{1-x-y}Ge_xC_y$ has less misfit strain and greater critical thickness than $Si_{1-x-y}Ge_x$ that is C-free. However, a corresponding increase in band gap, assuming the average band structure between Si−Ge and diamond as suggested by Soref, is not observed. In fact, for C concentrations of ~1 atom %, the band gap of $Si_{1-x-y}Ge_xC_y$ alloys has been found by photoluminescence to have a lower energy than that of $Si_{1-x}Ge_x$ with the same Si:Ge ratio (see Figure 19).[60] Nevertheless, HBTs have been fabricated using $Si_{1-x-y}Ge_xC_y$ and initial results indicate a slight increase in band gap (by 26 meV/% C).[61]

Photoluminescence studies have shown[52] that band gaps in strained $Si_{1-x}C_x$/Si quantum well structures decrease slightly with increasing C concentration up to ~1.5 atom % C. The band gap reduction in this system is, however, attributed to the large tensile strain that must exist within the alloy layers, and this lowers the energy of the D-electron valleys oriented in the growth direction. Based on these results, a prediction of the band structure was formulated, as shown schematically in Figure 20, and is compared with the corresponding structure of compressively strained $Si_{1-x}Ge_x$.[62] The fundamental gap is reduced and the main offset occurs in the conduction band, whereas the reduction in the $Si_{1-x}Ge_x$ system occurs in the valence band. This

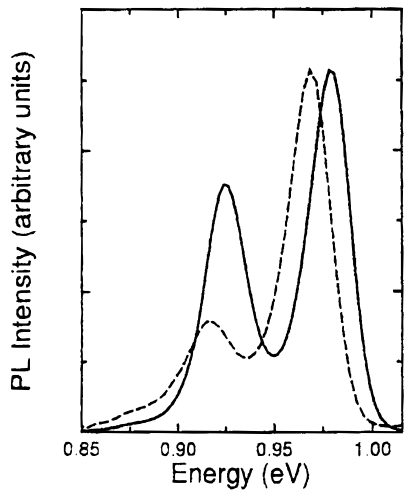

Figure 19. Low-temperature photoluminescence spectra from $Si_{0.79}Ge_{0.20}C_{0.01}$/Si (dotted line) and $Si_{0.80}Ge_{0.20}$/Si (solid line) grown by CVD.[60]

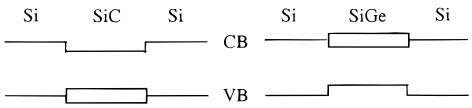

Figure 20. Schematic of band structure predicted for tensile-strained $Si_{1-x}C_x$ on Si in comparison with compressive-strained $Si_{1-x}Ge_x$.

feature is expected to have important implications for heterostructure engineering. Initial measurements also show surprisingly enhanced electron mobilities due to the presence of carbon in the $Si_{1-x}C_x$ system, in contrast to the standard reduction of mobility due to scattering observed in other alloy systems.[62]

Many groups can now deposit epitaxial $Si_{1-x-y}Ge_xC_y$ layers on Si with ~1.5% C content that display a well-identified, band-edge luminescence. Although theoretical studies of these systems remain uncertain and contradictory, a reasonable picture of the influence of substitutional C on the band gap and band alignment is beginning to emerge. The band offset of $Si_{1-x}C_x$/Si quantum wells is mainly in the conduction band, thus making the $Si_{1-x}C_x$/Si system an alternative to Si/SiGe. Superlattices of the type $Si_{1-x}Ge_x/Si_{1-x}C_x$ are attractive for optoelectronic applications. Laser emission in the SiGe(C)/Si quantum wells is considered a reasonable possibility. The development of novel HBTs with an SiGeC base has been reported,[61] and the expected advantage of reduced strain effects in the heterostructure has been satisfied. To achieve lattice matching and further influence the band structure, however, higher C concentrations are still required.

Summary

In this report we have described the development of simple inorganic precursors that provide the means for synthesis of completely new alloys and compounds in the Si−Ge−C system that cannot be obtained by other methods. Examples include strain-stabilized Si_4C, the microscopically strained $(Si_2Ge)C_x$, and $(Ge_2Si)C_x$ as well as strained or completely relaxed carbide nanostructures in the Ge−C system. Their utilization in the heteroepitaxial growth of Si−Ge−C and related alloys has pushed the solubility limit of C in SiGe, Ge and Si well beyond the levels already achieved by conventional synthetic routes. These precursors are expected to have substantial impact in the further useful development of these technologically important systems. The newly developed family of inorganic compounds $C(GeX_3)_4$, where X = H, Cl, and Br, is not only a practical source of precursors for materials synthesis but they also provide important bonding information with regard to structural characterization and theoretical modeling of crystalline semiconductor systems.

Acknowledgment. Much of the work described here was supported by the National Science Foundation (Grant DMR 9458047). The support of Si−C-related work by the Army Research Office (ARO) Grant no. DAAH04-96-1-0229 is gratefully acknowledged.

References

(1) Kasper, E. *Physica Scripta* **1991**, *35*, 232.
(2) (a) Bergman, C.; Chastel, R.; Castanel, R. *J. Phase Equilibr.* **1992**, *13*, 113. (b) Dismukes, J. P.; Ekstrom, L.; Paff, R. J. *J. Phys. Chem.* **1964**, *68*, 3021.
(3) Jain, S. C. *Germanium−Silicon Strained Layers and Heterostructures*; Academic: Boston, 1994.
(4) Powell, A. R.; Eberl, K.; Ek, B. A.; Iyer, S. S. *J. Cryst. Growth* **1993**, *127*, 425.
(5) (a) Strane, J. W.; Stein, H. J.; Lee, S. R.; Doyle, B. L.; Picraux, S. T.; Mayer, J. W. *Appl. Phys. Lett.* **1993**, *63*, 2786. (b) Atzmon, Z.; Bair, A. E.; Jaquez, J.; Mayer, J. W.; Chandrasekhar, D.; Smith, D. J.; Hervig, R. L.; Robinson, McD. *Appl. Phys. Lett.* **1994**, *65*, 2559.
(6) Iyer, S. S.; Eberl, K.; Goursky, M. S.; LeGoues, F. K.; J. C. Tsang, J. C. *Appl. Phys. Lett.* **1992**, *60*, 356.
(7) Chang, C. L.; Amour, A. St.; Strum, J. C. *Appl. Phys. Lett.* **1997**, *70*, 1557.
(8) Kouvetakis, J.; Nesting, D.; Smith, D. *J. Am. Chem. Soc.* Book Ser., in press.
(9) Todd, M.; Matsunaga, P.; Kouvetakis, J.; Smith, D. J. *Appl. Phys. Lett.* **1995**, *67*, 1247.
(10) Soref, R. A. *J. Appl. Phys.* **1991**, *70*, 2470.
(11) Demkov, A. A. *Phys. Rev. B* **1993**, *48*, 2207.
(12) (a) Hager, R.; Steigelman, O.; Muller, G.; Schmidbaur, H.; Robertson, H. H.; Rankin, D. W. *Angew. Chem., Int. Ed.* **1990**, *29*, 201, 1524. (b) Schmidbaur, H.; Zech, J. *Eur. J. Solid State Chem.* **1992**, *29*, 5. (c) Beyer, W.; Hager, R.; Schmidbaur, H.; Winterling, G. *Appl. Phys. Lett* **1989**, *54*, 1666. (d) Schmidbaur, H.; Rott, J.; Reber, G.; Muller, G. *Z. Naturforsch.* **1998**, *43b*, 726; **1990**, *45b*, 961. (e) Hager, R.; Steigelman, O.; Muller, G.; Schmidbaur, H. *Chem. Ber.* **1989**, *122*, 2115.
(13) Matsunaga, P. T.; Kouvetakis, J.; Groy, T. L. *Inorg. Chem.* **1995**, *34*, 5103.
(14) Haaland, A.; Shorokhov, D. P.; Strand, T. G.; Kouvetakis, J.; O'Keeffe, M. *Inorg. Chem.* **1997**, *36*, 5198.
(15) Hoffman, L.; Bach, J. C.; Nielsen, B. B.; Jones, R.; Leary, P.; Oberg, S. *Phys. Rev. B* **1997**, 11167.
(16) Tersoff, J. *Phys. Rev. B* **1989**, *39*, 5556.
(17) Adams, G. B.; O'Keeffe M.; Kouvetakis, J.; Sankey, O. F., unpublished results.
(18) Kouvetakis, J.; Haaland, A.; Shorokhov, D.; Matsunaga, P. *J. Am. Chem. Soc.* **1998**, *120*, 6738.
(19) Tollman, J. J.; Frost, A. A.; Topiol, S.; Jacobson, S.; Ratner, M. A. *Theor. Chim. Acta* **1981**, *58*, 285.
(20) Ourmazd, A.; Bean, J. C. *Phys. Rev. Lett.* **1985**, *55*, 765.
(21) Hull, R. *Bull. Am. Phys. Soc.* **1986**, *30*, 265.
(22) Berding, M. A.; Sher, A.; van Schilfgaarde, M. *Phys. Rev. B* **1997**, *56*, 3885.
(23) Kouvetakis, J.; Nesting, D.; O'Keefee. M.; Smith, D. J. *Chem. Mater.* **1998**, *10*, 1396.
(24) Kouvetakis, J.; Todd, M.; Chandrasekhar, D.; Smith, D. J. *Appl. Phys. Lett.* **1994**, *65*, 2960.
(25) Rucker, H.; Methfessel, M.; Bugiel, E.; Osten, A. J. *Phys. Rev. Lett.* **1994**, *72*, 3578.
(26) O'Keefee, M., unpublished results.
(27) Martins, J. L.; Zunger, A. *Phys. Rev. Lett.* **1986**, *56*, 1400.
(28) Flynn, C. P. *Phys. Rev. Lett.* **1986**, *57*, 599.
(29) Guedj, C.; Portier, X.; Hairie, A.; Bouchier, D.; Calvarin, G.; Picrou, B. *Thin Solid Films* **1997**, *294*, 129.
(30) Kouvetakis. J.; Chandrasekhar, D.; Smith, D. J. *Appl. Phys. Lett.* **1998**, *72*, 930.
(31) Newman, R. C.; Willis, J. B. J. *J. Phys. Chem. Solids* **1965**, *26*, 373.

(32) Kajiyama, H.; Muramatsu, S.; Shimada, T.; Nishino, Y. *Phys. Rev. B* **1992**, *45*, 14005.
(33) LeGoues, F. K.; Kesan, V. P.; Iyer, S. S. *Phys. Rev. Lett.* **1990**, *64*, 40.
(34) LeGoues, F. K.; Kesan, V. P.; Iyer, S. S.; Tersoff, J.; Tromp, R. *Phys. Rev. Lett.* **1990**, *64*, 2038.
(35) Chang, J. C.; Kesan, V. P.; Freouf, J. L.; Le Goues, F. K.; Iyer, S. S. *Phys. Rev. Lett.* **1992**, *46*, 6907.
(36) Zhong, P.; Zheng, Y.; Zhang, R.; Hu, L. *Appl. Phys. Lett.* **1992**, *61*, 80.
(37) Lebedev, O. I.; Kiselev, N. A.; Vasiliev, A. G.; Orlikovsky, A. A. *Inst. Phys., Conf. Ser.* **1995**, *14G*, 297.
(38) (a) Patton, G. L.; Harame, D. L.; Strock, J. M.; Mayerson, B. S.; Scilla, G. S. *I EEE Electron Device Lett.* **1989**, *10*, 534. (b) Patton, G. L.; Comfort, J. H.; Meyerson, B. S.; Crabbe, E. F.; Scilla, G. J.; Strock, J. M. C.; Sun, J. Y. C.; Harame, D. L.; Burghartz, J. N. *IEEE Electron Device Lett.* **1990**, *11*, 171. (c) Crabbé, E. F.; Comfort, J. H.; Lee, W.; Gressler, J. D.; Meyerson, B. S.; Megdanis, A. C.; Sun, J. Y. C.; Strock, J. M. C. *IEEE Electron Device Lett.* **1992**, *13*, 259.
(39) Grouhle, A.; Schuppen, A. *Thin Solid Films* **1997**, *294*, 246.
(40) Compound Semiconductors, Nov./Dec. 1995.
(41) Laursen, T.; Chandrasekhar, D.; Smith, D. J.; Mayer, J. W.; Hoffman, J.; Westhoff, R.; Robinson, McD. *Appl. Phys. Lett.* **1997**, *71, 1634.*
(42) Atzmon, Z.; Bair, A. E.; Jaquez, J.; Mayer, J. W.; Chandrasekhar, D.; Smith, D. J.; Hervig, R. L.; Robinson, McD. *Appl. Phys. Lett.* **1994**, *65*, 2559.
(43) Iyer, S. S.; Patton, G. L.; Stork, J. M.; Meyerson, B. S.; Harame, D. L. *IEEE Trans. Electron. Dev.* **1989**, *36*, 2043.
(44) Sankey, O. F.; Demkov, A. A.; Petuskey, W. T.; McMillan P. F. *Model Simul. Mater. Sci. Eng.* **1993**, *1*, 741.
(45) None appears in the Inorganic Crystal Structure Database, Gmelin Institute fur anorganische Chemie, Karlsruhe Germany, 1996.
(46) (a) Osten, H. J.; Bugiel, E.; Zaumseil, P. *J. Cryst. Growth* **1994**, *142*, 322. (b) Osten, H. J.; Klatt, J. *Appl. Phys. Lett.* **1994**, *65*, 2960.
(47) Kolodzey, J.; O'Neil, P. A.; Zhang, S.; Orner, B. A.; Roe, K.; Unruh, K. M.; Swann, C. P.; Waite, M. M.; Ismat Shah, S. *Appl. Phys. Lett.* **1995**, *67*, 1865.
(48) Todd, M.; Kouvetakis, J.; Smith, D. J., unpublished results.
(49) Todd, M.; McMurran, J.; Kouvetakis, J.; Smith, D. J. *Chem. Mater.* **1996**, *8*, 2491.
(50) Nozaki, T.; Yatsurugi, Y.; Akiyama, N. *J. Electrochem. Soc.* **1970**, *117*, 1566.
(51) Posthill, J. B.; Rudder, R. A.; Fattangandy, S. V.; Fountain, G. G.; Markunas R. J. *Appl. Phys. Lett.* **1990**, *56*, 734.
(52) Brunner, K.; Eberl, K.; Winter, W. *Phys. Rev. Lett.* **1996**, *76*, 303.
(53) Iyer, S. S.; Eberl, K.; Goorsky, M. S.; LeGoues, F. K.; Chang, J. C.; Gardone, F. *Appl. Phys. Lett.* **1992**, *60*, 356.
(54) (a) Kissinger, W.; Osten, H. J.; Weidner, M.; Eichler, M. *J. Appl. Phys.* **1996**, *79*, 3016. (b) Strane, W.; Stein, H. J.; Lee, S. R. Picraux, S. T.; Watanabe, J. K.; Mayer, J. W. *J. Appl. Phys.* **1994**, *76*, 3656.
(55) Chandrasekhar, D.; McMurran, J.; Smith, D. J.; Kouvetakis, J.; Lorentzen, J. D.; Menendez, J. *Appl. Phys. Lett.*, in press.
(56) Mitchel, T. O.; Hoyt, J. L.; Gibbons, J. F. *Appl. Phys. Lett.* **1997**, *71*, 1688;.
(57) Melendez-Lira, M.; Menendez, J.; Kramer, K. M.; Thomson, M. O.; Cave, N.; Liu, R.; Christiansen, J. W.; Theodore, N. D.; Candaleria, J. J. *Phys. Rev B* **1997**, *56*, 4246.
(58) Kissinger, W.; Osten, H. J.; Weidner, M.; Eichler, M. *Appl. Phys. Lett.* **1996**, *79*, 3648.
(59) Rim, K.; Takagi, S.; Welser, J. J.; Hoyt, J. L.; Gibson, J. F. *Mater. Res. Symp. Proc.* **1995**, *379*, 327.
(60) Lorentzen, J. D.; Loechelt, G. H.; Melendez-Lira, M.; Menendez, J.; Sego, S.; Culbertson, R. J.; Windl. W.; Sankey, O. F., Bair, A. E.; Alford, T. L. *Appl. Phys. Lett.* **1997**, *70*, 2353.
(61) Amour, A. St.; Lanzerotti, L. D.; Chang, C. L.; Strum, J. C. *Thin Solid Films* **1997**, *294*, 112.
(62) Osten, H. J.; Kim, M.; Lippert, G.; Zaumseil, P. *Thin Solid Films* **1997**, *294*, 93.

CM980294B